Medicinal Chemistry Research
https://doi.org/10.1007/s00044-020-02560-1

MEDICINAL CHEMISTRY RESEARCH

ORIGINAL RESEARCH

Synthesis and biological evaluation of selected 7-azaindole derivatives as CDK9/Cyclin T and Haspin inhibitors

Lianie Pieterse[1] · Lesetja J. Legoabe[1] · Richard M. Beteck[1] · Béatrice Josselin[2,3] · Stéphane Bach[2,3] · Sandrine Ruchaud[2]

Received: 28 March 2020 / Accepted: 7 May 2020

Abstract

The 7-azaindole scaffold attracts attention due to its value in the design of inhibitors of diseases related protein kinases. However, this scaffold has not been evaluated against Haploid germ cell-specific nuclear protein kinase (Haspin). Herein, we report the synthesis of a select set of 7-azaindole derivatives and their evaluation against Haspin. The compounds were also evaluated against CDK9/Cyclin T kinase. The synthesis of 7-azaindole derivatives was achieved through Suzuki coupling using appropriate halogenated 7-azaindole and boronic acids. Seven of the screened compounds exhibited activity as CDK9/Cyclin T and/or Haspin inhibitors in a nanomolar to low micromolar range. The most promising dual inhibiting compound **18c**, exhibited an inhibitory potential of 0.206 µM against CDK9/Cyclin T and 0.118 µM against Haspin. The dual inhibition of CDK9/Cyclin T and Haspin could afford a potentially potent antimitotic agent of value in further anticancer studies.

Keywords Protein kinases · 7-Azaindole · anticancer · CDK9/ Cyclin T · Haspin

Introduction

The majority of the manifold cellular processes in the human body are vastly dependent on a superfamily of homologous proteins, known as protein kinases (PKs) (Hanks and Hunter 1995; Hunter 1995). The PKs that make up the human kinome tally up to a total of 518 PKs, thus accounting for 1.7% of human genes (Manning et al. 2002) and are integrally linked to the process of protein phosphorylation which regulates signal transduction, as these proteins facilitate the transfer of phosphoryl groups from phosphate donors such as ATP, to receptor substrates that range from small molecules to lipids and proteins (Lawson et al. 2016). Signal transduction, in turn is linked to cell growth, metabolism, differentiation and apoptosis (Liao 2007). Therefore, any dysregulation of PKs (such as overexpression) could result in serious ramifications, the likes of which include, cell transformation and cancer, inflammation, diabetes and neurodegenerative diseases like Alzheimer's disease (Flight 2013; Huse and Kuriyan 2002; Noh and King 2007). Hence, PKs have become appealing targets for drug discovery, even being touted as the second most important drug targets after G-protein-coupled receptors (Cohen 2002).

This forms the backdrop against which the discovery of novel PK inhibitors plays out and indeed, a number of kinase inhibitors are in clinical use or undergoing clinical trials, like imatinib, for the treatment of chronic myelogenous leukaemia (CML) and trastuzumab in breast cancer (Fedorov et al. 2010). Nevertheless, these inhibitors target only a slight portion of the kinome and numerous clinically relevant kinases still remain relatively underexplored (Duong-Ly and Peterson 2013).

One such PK is the Haploid germ cell-specific nuclear protein kinase (Haspin). Haspin has only recently been added to the ranks of known PKs and is thought to phosphorylate histone H3 during mitosis (Higgins 2010).

Supplementary information The online version of this article (https://doi.org/10.1007/s00044-020-02560-1) contains supplementary material, which is available to authorized users.

✉ Lesetja J. Legoabe
lesetja.legoabe@nwu.ac.za

[1] Centre of Excellence for Pharmaceutical Sciences, North-West University, Private Bag X6001, Potchefstroom 2520, South Africa

[2] Sorbonne Université, CNRS, UMR 8227, Integrative Biology of Marine Models Laboratory (LBI2M), Station Biologique de Roscoff, CS 90074, 29680 Roscoff Cedex, France

[3] Sorbonne Université, CNRS, FR2424, Plateforme de criblage KISSf (Kinase Inhibitor Specialized Screening facility), Station Biologique de Roscoff, CS90074, 29680 Roscoff Cedex, France

Published online: 22 May 2020

It is believed that identification of Haspin inhibitors might supply valuable candidates for biological studies and cancer treatment. This belief stems from the following factors: (i) Haspin is deemed important in the regulation of mitosis and Haspin RNAi in tumour cell lines thwarts chromosome alignment and completion of the normal mitotic process (Dai et al. 2005; Dai et al. 2006). This suggests that Haspin inhibitors have the potential to act as novel antimitotic agents with an aptitude for halting the proliferation of cancer cells (de Cárcer et al. 2007; Schmidt and Bastians 2007). (ii) Haspin mRNA is predominantly expressed in proliferative cells and not in non-dividing cells, making it another attractive target for cancer treatment (Higgins 2001a, b). (iii) Not only is the primary sequence of Haspin structurally different to that of other known kinases, but it also does not fit into any of the known eukaryotic kinase families and humans appear to have only one Haspin homologue, indicating that the design of highly selective Haspin inhibitors is probable (Higgins 2003; Higgins 2001a, b; Kannan et al. 2007). Thus, designing a study that aims to explore the Haspin target, may yield valuable novel knowledge in the field of PK inhibition and treatment of disease.

In general, PK inhibitors are largely designed to bind to the ATP binding site situated within the deep cleft between the N- and C-terminal lobes of the kinase catalytic domain. Binding is generally the product of hydrogen bond interactions with the hinge region that connects the two lobes (Liao 2007), and as such, the 7-azaindole scaffold (**1**) has been highlighted as a prime candidate for targeting PKs because of the scaffolds enhanced fit within the ATP binding site:

the pyridine N serves as a hydrogen bond acceptor, while the NH of the pyrrole ring acts as a hydrogen bond donor, together they form bidentate hydrogen bonds with the hinge region of the kinase (Irie and Sawa 2018; Mérour et al. 2014; Zuccotto et al. 2009). Therefore, it is hardly surprising that in recent years, the 7-azaindole scaffold has been widely explored in terms of PK inhibition and a few examples of PK successfully inhibited using the 7-azaindole scaffold include: anaplasmic lymphoma kinase (ALK) (Gummadi et al. 2013), the aurora kinases (Bavetsias et al. 2013), cell division cycle 7 kinase (Cdc 7) (Harrington et al. 2013), C-Met kinase (Kim et al. 2008), DYRK1A (Gourdain et al. 2013), focal adhesion kinase (FAK) (Heinrich et al. 2013), IκK kinase(IKK) (Liddle et al. 2009), KIT/FMS dual kinase (Zhang et al. 2013), p38α mitogen-activated protein kinase (p38α MAP) (Mavunkel et al. 2010), proto-oncogene serine/threonine-protein kinase 1 (PIM1) (Nakano et al. 2012), mammalian target of rapamycin kinase (m-TOR) (Tsou et al. 2010), tropomyosin-related kinase A (TrkA) (Hong et al. 2012) (see Fig. 1).

It is important to note that the 7-azaindole scaffold has never been explored for Haspin inhibition. Prompted by the relative novelty of the Haspin target and the general success of the 7-azaindole scaffold in PK inhibition, twenty-four 7-azaindole derivatives (divided into two series: 4-substituted 7-azaindoles and 5-substituted 7-azaindoles, see Tables 1 and 2), were synthesised and evaluated in vitro as potential Haspin inhibitors. The compounds were selected for their simplicity and comparatively inexpensive method of synthesis, while also being novel to the Haspin target. A SciFinder search of each compound was conducted to determine the novelty of each compound. Compounds **18c, 18f, 18h, 18i, 19e, 19l** and **19o** had no known references in SciFinder and are deemed novel. In turn, compounds **18a** (Metz et al. 2011), **18b** (Arnold et al. 2007), **18d** (Ledeboer et al. 2006), **18e** (Allegretti et al. 2001) and **18g** (Ibrahim et al. 2007), **19a** (Ibrahim et al. 2007), **19b** (Huang et al. 2019), **19c** (Ibrahim et al. 2007), **19d** (Huang et al. 2019), **19f** (Ibrahim et al. 2007), **19g** (Huang et al. 2019), **19h** (Huang et al. 2019), **19i** (Huang et al. 2019), **19j** (Liu et al. 2019), **19k** (Huang et al. 2019), **19m** (Ibrahim et al. 2007) and **19n** (Ibrahim et al. 2007) have previously featured in literature. Alongside Haspin, the derivatives were screened against other PKs: (i) *Hs*CDK$_2$/Cyclin A, (ii) *Hs*CDK$_5$/p25, (iii) *Hs*CDK$_9$/Cyclin T, (iv) *Hs*Pim-1, (v) *Ssc*CK1δ/ε, (vi) *Ssc*GSK3α/β and (vii) *Lm*CK1.

Materials and methods

All compounds were synthesised according to the general methods discussed in the experimental section. Starting materials were procured from AK Scientific, CHR-6494 and flavopiridol were purchased from Sigma Aldrich and were used without further purification, unless otherwise specified. Proton (1H) and carbon (13C) nuclear magnetic resonance (NMR) spectra were recorded by means of a Bruker Avance III 600 spectrometer at frequencies of 600 MHz and 151 MHz, respectively, in deuterated dimethylsulfoxide (DMSO-d6). The chemical shifts (δ) are reported in parts per million (ppm) and internally referenced to the signal of tetramethylsaline (TMS). Spin multiplicities are indicated as follow: s (singlet), d (doublet), dd (doublet of doublets), td (triplet of doublets), t (triplet), q (quartet) and m (multiplet). Coupling constants (*J*) are reported in Hz. High resolution mass spectra (HRMS) were recorded by means of a Bruker micrOTOF-Q II mass spectrometer in atmospheric pressure chemical ionisation (APCI) mode (positive ion polarity). High performance liquid chromatography (HPLC) analyses were performed by means of an Agilent 1100 HPLC system, using a Venusil XBP C18(2) (4.6 mm ×150 mm) 5 µM column with mobile phase A (water + 0.1% formic acid) and mobile phase B (acetonitrile + 0.1% formic acid)

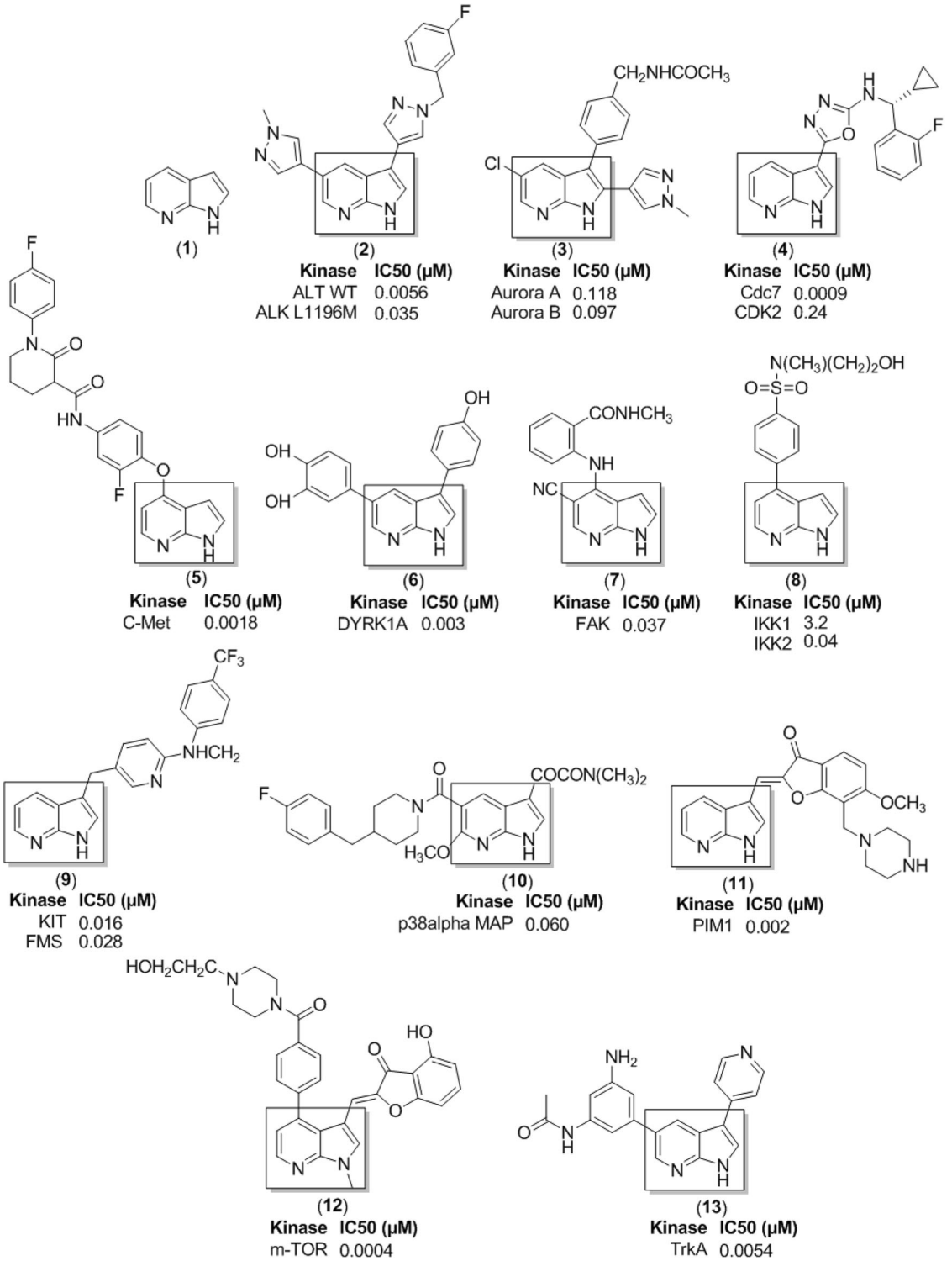

Fig. 1 A depiction of several compounds bearing the 7-azaindole structure known to inhibit various PKs. References: (**2**)(Gummadi et al. 2013), (**3**) (Bavetsias et al. 2013), (**4**) (Harrington et al. 2013), (**5**) (Kim et al. 2008), (**6**) (Gourdain et al. 2013), (**7**) (Heinrich et al. 2013), (**8**) (Liddle et al. 2009), (**9**) (Zhang et al. 2013), (**10**) (Mavunkel et al. 2010), (**11**) (Nakano et al. 2012), (**12**) (Tsou et al. 2010), (**13**) (Hong et al. 2012)

against a gradient of 50% B (0–2 min), 100% B (2–8 min), 100% B (8–11 min), 50% B (11–11.1 min) and 50% B (11.1–13 min) at 22 °C. Melting points (mp) were determined by a Buchi B545 melting point apparatus and are uncorrected. Thin layer chromatography (TLC) was accomplished using silica gel 60 TLC plates (Merck) and a

Table 1 Table depicting synthesis of 4-substituted 7-azaindole derivative, target compounds, and yields achieved

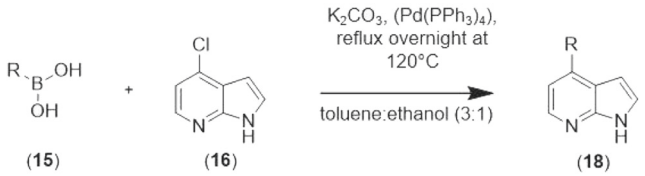

(15) (16) (18)

Compound	Yield (%)	Compound	Yield (%)	Compound	Yield (%)
(18a)	42	(18d)	38	(18g)	75
(18b)	39	(18e)	34	(18h)	39
(18c)	29	(18f)	63	(18i)	59

UV254 fluorescent indicator to determine retention factor (Rf) using petroleum ether: ethyl acetate (1:1) as eluent.

Experimental

Chemistry

Numerous 4-, and 5-substituted 7-azaindole derivatives were prepared by means of Suzuki-Miyaura cross coupling between either 4-chloro-1*H*-pyrrolo[2,3-*b*]pyridine or 5-bromo-1*H*-pyrrolo[2,3-*b*]pyridine and an assortment of commercially available boronic acids in a single step reaction. Suzuki coupling affords an excellent platform for carbon-carbon bond formation and entails a palladium-catalysed cross-coupling reaction between organoboron compounds and organic halides or triflates (Kim et al. 2002; Wolfe and Buchwald 1999). Tetrakis(triphenylphosphine)palladium(0) ($Pd(PPh_3)_4$) served as the catalyst and the two series (4-substituted and 5-substituted 7-azaindole derivatives) were obtained in varying yields of 11-82%. (see Table 1 and Table 3). Synthesis of the 5-substituted 7-azaindole derivatives (**20a** – **20o**) proceeded smoothly as per standard literature methods (Littke and Fu 2002). Noteworthy, although the reaction for the 4-substituted 7-azaindole derivatives was performed with the same basic reagents, the reaction of 4-chloro-7-azaindole and appropriate boronic acid required a greater ratio of boronic acid (at least 4 equivalences of azaindole) for successful coupling. Thus, a total of 24 compounds were produced according to conditions discussed above. The synthesised compounds were confirmed by NMR and HRMS analysis.

General synthetic procedure for the selected 7-azaindole derivatives Compounds **18a–19o** were synthesised by means of Suzuki coupling (also known as Suzuki-Miyaura coupling) under nitrogen atmosphere. To a stirred solution of either 4-chloro-7-azaindole for series 1 or 5-bromo-7-

Table 2 Percentage of residual activity for compounds **18a–b** and **19a–m** at 1 and 10 μM using a representative kinase panel

Cpd	*Hs* CDK2/ CyclinA	*Hs* CDK5/ p25	*Hs* CDK9/ CyclinT	*Hs* Haspin	*Hs* PIM1	*Ssc* CK1δ/ε	*Ssc* GSK3α/ β	*Lm* CK1
18a	64 (99)	66 (91)	***5 (10)***	***19 (95)***	50 (81)	54 (83)	70 (89)	72 (80)
18b	81 (97)	62 (≥100)	***9 (26)***	***14 (29)***	66 (99)	71 (86)	70 (91)	91 (96)
18c	73 (73)	53 (82)	***14 (30)***	***10 (21)***	***10 (35)***	79 (89)	78 (91)	79 (≥100)
18d	59 (99)	83 (≥100)	***15 (44)***	58 (63)	90 (98)	87 (86)	75 (91)	46 (62)
18e	53 (77)	6 (78)	***6 (11)***	***15 (30)***	60 (≥100)	67 (95)	87 (93)	63 (85)
18f	59 (≥100)	54 (75)	**10 (26)**	***20 (47)***	***20 (39)***	79 (95)	73 (≥100)	94 (99)
18g	≥100 (91)	71 (≥100)	24 (74)	***18 (73)***	29 (99)	82 (≥100)	73 (≥100)	70 (79)
18h	63 (71)	79 (96)	***3 (15)***	***8 (28)***	77 (87)	76 (86)	78 (86)	41 (56)
18i	≥100 (89)	98 (≥100)	70 (82)	73 (83)	≥100 (≥100)	93 (95)	≥100 (89)	19 (44)
19a	24 (77)	45 (61)	31 (94)	41 (73)	80 (≥100)	27 (57)	51 (86)	37 (≥100)
19b	63 (88)	75 (89)	54 (81)	50 (71)	≥100 (≥100)	55 (90)	68 (94)	66 (82)
19c	61 (≥100)	68 (≥100)	44 (62)	32 (64)	59 (≥100)	47 (84)	89 (91)	99 (81)
19d	≥100 (94)	78 (≥100)	78 (63)	50 (59)	46 (≥100)	68 (78)	96 (95)	56 (69)
19e	90 (≥100)	89 (94)	47 (69)	85 (71)	≥100 (77)	66 (79)	86 (94)	75 (66)
19f	78 (88)	50 (86)	60 (74)	71 (76)	31 (≥100)	59 (71)	88 (97)	52 (82)
19g	37 (79)	63 (93)	74 (63)	49 (56)	≥100 (≥100)	48 (67)	78 (71)	63 (≥100)
19h	79 (≥100)	75 (≥100)	54 (88)	43 (53)	≥100 (≥100)	61 (77)	66 (98)	61 (≥100)
19i	93 (≥100)	≥100 (≥100)	92 (≥100)	79 (81)	50 (78)	92 (99)	94 (≥100)	≥100 (≥100)
19j	65 (87)	64 (≥100)	71 (89)	≥100 (97)	83 (87)	72 (88)	71 (97)	≥100 (≥100)
19k	68 (93)	≥100 (88)	89 (73)	77 (62)	≥100 (98)	71 (63)	93 (78)	≥100 (61)
19l	≥100 (91)	84 (≥100)	72 (73)	73 (90)	≥100 (≥100)	69 (78)	83 (95)	36 (88)
19m	99 (≥100)	77 (93)	49 (81)	40 (64)	37 (58)	58 (89)	86 (92)	71 (83)
19n	61 (87)	***20 (≥100)***[a]	21 (56)	***7 (29)***	39 (55)	49 (73)	60 (92)	62 (90)
19o	79 (≥100)	98 (≥100)	74 (81)	47 (52)	56 (≥100)	64 (81)	77 (93)	≥100 (≥100)[a]

Values represent the percentage of residual kinase activity for compounds used at 10 μM and 1 μM concentrations. The values obtained with compounds at 1 μM are in bracket. The most significant results are presented in bold-italic. Activities were assessed in duplicate using 10 μM ATP.

azaindole for series 2 (1.523 mmol), in 25 mL of a 3:1 toluene: ethanol mixture, ($Pd(PPh_3)_4$) (0.023 mmol) and 1.6 mL of a 2 M K_2CO_3 solution, the appropriate boronic acid (1.523 mmol for series 1 and 6.092 mmol for series 2) was added. Followed by additional 0.5 mmol additions if deemed necessary during monitoring of TLC plates. The reaction mixture was stirred continuously under reflux (120°C) for at least 24 h and then monitored via TLC until complete. Subsequently, the reaction mixture was allowed to cool to room temperature and the solvent was removed under reduced pressure. The resulting residue was extracted with distilled water and dichloromethane (3 × 25 mL). The organic layers were combined and dried with $MgSO_4$. The solvent was once again removed under reduced pressure and the resulting product was recrystallized from a suitable solvent.

Physical properties and characterization The NMR spectra of 4/5-Halo-7-azaindole—starting material distinctly bears 7 carbons and 5 hydrogens peaks. The proton NMR spectra of 4/5-Phenyl-7-azaindole derivatives: the target compounds bear no hydrogen on C4 in the case of 4-substituted compounds, or C5 in the case of 5-substituted compounds and the presence of additional aromatic signals suggest that aromatic moieties were successfully coupled. Furthermore, the singlet at approximately 12 ppm in ^{1}H-NMR is assignable to N-H, this signifies that no reaction took place at NH-position (position 1). The NMR spectra and other characterisation data can be found in the Supporting information.

*4-Phenyl-1H-pyrrolo[2,3-b]pyridine (**18a**)*: compound was synthesised from phenylboronic acid and 4-chloro-7-azaindole in a yield of 42.37%, recrystallized from acetonitrile, dark beige crystals, mp 208 – 210 °C, Rf = 0.48 (1 petroleum ether: 1 ethyl acetate). ^{1}H NMR (DMSO-d_6, 600 MHz) δ 11.86 (1H, s, NH), 8.33 (1H, d, $J = 4.8$ Hz, H-6), 7.81 (2H, d, $J = 7.6$ Hz, H-2′,H-6′), 7.60 (3H, m, H-2, H-3′, H-5′), 7.50 (1H, t, $J = 7.3$ Hz, H-4′), 7.23 (1H, d, $J =$ 4.8 Hz, H-5), 6.68–6.63 (1H, m, H-3). ^{13}C NMR (DMSO-d_6, 150 MHz) δ 149.6 (C-7a), 143.4 (C-6), 140.7 (C-1′),

Table 3 A table depicting 5-substituted 7-azaindole derivative synthesis, compounds synthesised and yields achieved

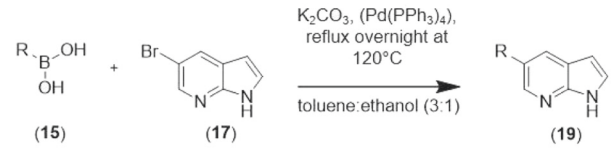

(**15**) (**17**) (**19**)

Compound	Yield (%)	Compound	Yield (%)	Compound	Yield (%)
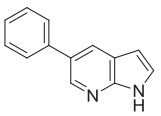 (**19a**)	63	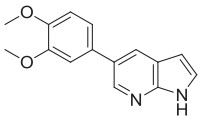 (**19f**)	46	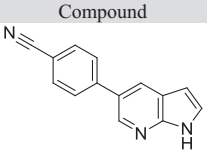 (**19k**)	34
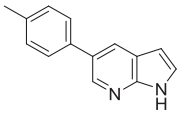 (**19b**)	60	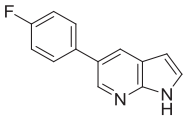 (**19g**)	53	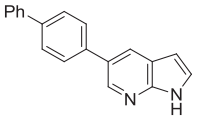 (**19l**)	20
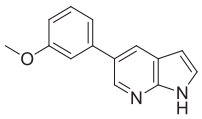 (**19c**)	63	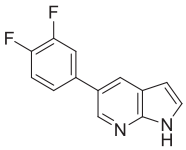 (**19h**)	43	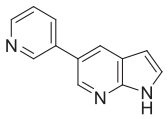 (**19m**)	45
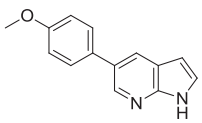 (**19d**)	83	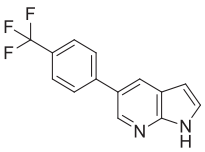 (**19i**)	53	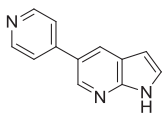 (**19n**)	45
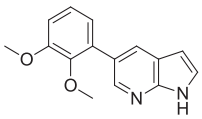 (**19e**)	11	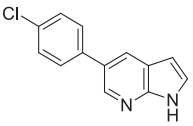 (**19j**)	42	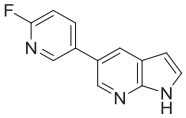 (**19o**)	61

139.0 (C-4), 129.5 (C-3′, C-5′), 128.8 (C-3a), 128.7 (C-2′, C-6′), 127.1 (C-4′), 117.7 (C-2), 114.7 (C-5), 99.4 (C-3). APCI-HRMS *m/z*: calc. for $C_{13}H_{11}N_2$ (MH^+), 195.0916, found 195.0920; Purity (HPLC): 98% (column: Venusil XBP C18(2) 4.6 mm ×150 mm; retention time: 15 min).

4-(4-Methylphenyl)-1H-pyrrolo[2,3-b]pyridine (***18b***): compound was synthesised from 4-methylphenylboronic acid and 4-chloro-7-azaindole in a yield of 38.80%, recrystallized from acetonitrile, yellow powder, mp 169–171 °C, Rf = 0.38 (4 petroleum ether: 1 ethyl acetate). ^{1}H NMR (DMSO-d_6, 600 MHz) δ 11.78 (1H, s, NH), 8.27 (1H, d, J = 4.7 Hz, H-6), 7.67 (2H, d, J = 7.9 Hz, H-2′, H-6′), 7.53 (1H, d, J = 2.9 Hz, H-2), 7.36 (2H, d, J = 7.7 Hz, H-3′-H-5′), 7.16 (1H, d, J = 4.7 Hz, H-5), 6.60 (1H, d, J = 2.9 Hz, H-3), 2.39 (3H, s, Me-4′). ^{13}C NMR (DMSO-d_6, 150 MHz) δ 149.6 (C-7a), 143.4 (C-6), 140.7 (C-4′), 138.3 (C-1′), 136.1 (C-4), 130.0 (C-3′, C-5′), 128.6 (C-2′, C-6′), 126.9 (C-3a), 117.7 (C-2), 114.5 (C-5), 99.5 (C-3), 21.3 (Me-4′). APCI-HRMS *m/z*: calc. for $C_{14}H_{13}N_2$ (MH^+), 209.1073, found 209.1067; Purity (HPLC): 97% (column: Venusil XBP C18(2) 4.6 mm ×150 mm; retention time: 9 min).

0.4-(4-Methoxyphenyl)-1H-pyrrolo[2,3-b]pyridine (***18c***): compound was synthesised from 4-methoxyphenylboronic acid and 4-chloro-7-azaindole in a yield of 29.33%, recrystallized from acetonitrile, pale yellow powder, mp 212–212 °C, Rf = 0.18 (2 petroleum ether: 1 ethyl acetate). ^{1}H NMR (DMSO-d_6, 600 MHz) δ 11.75 (1H, s, NH), 8.25 (1H, d, J = 4.8 Hz, H-6), 7.73 (2H, d, J = 8.5 Hz, H-2′, H-6′), 7.52 (1H, t, J = 2.8 Hz, H-2), 7.14 (1H, d, J = 4.4 Hz, H-5), 7.12 (2H, d, J = 8.6 Hz, H-3′, H-5′), 6.61 (1H, d, J = 2.9 Hz, H-3), 3.84 (3H, s, MeO-4′). ^{13}C NMR (DMSO-d_6, 150 MHz) δ 159.9 (C-4′), 149.6 (C-7a), 143.4 (C-6), 140.5 (C-1′), 131.2 (C-4), 129.9 (C-2′, C-6′), 126.8 (C-3a), 117.5 (C-2), 114.9 (C-3′, C-5′), 114.3 (C-5), 99.5 (C-3), 55.7 (MeO-4′). APCI-HRMS *m/z*: calc. for $C_{14}H_{13}N_2O$ (MH^+),

225.1022, found 225.1017; Purity (HPLC): 99% (column: Venusil XBP C18(2) 4.6 mm × 150 mm; retention time: 7 min).

4-(2,3-Dimethoxyphenyl)-1H-pyrrolo[2,3-b]pyridine ***(18d)***: compound was synthesised from 2,3-dimethoxyphenylboronic acid and 4-chloro-7-azaindole in a yield of 37.73%, recrystallized from acetonitrile, sand coloured powder, mp 191–192 °C, Rf = 0.16 (4 petroleum ether: 1 ethyl acetate). 1H NMR (DMSO-d_6, 600 MHz) δ 11.69 (1H, s, NH), 8.24 (1H, d, J = 4.8 Hz, H-6), 7.47–7.44 (1H, m, H-2), 7.18 (1H, t, J = 7.8 Hz, H-5′), 7.14 (1H, dd, J = 8.6, 1.2 Hz, H-4′), 7.05 (1H, d, J = 5.1 Hz, H-5), 6.99 (1H, dd, J = 7.4, 1.0 Hz, H-6′), 6.25 (1H, 3, H-3), 3.87 (3H, s, MeO-2′), 3.48 (3H, s, MeO-3′). ^{13}C NMR (DMSO-d_6, 150 MHz) δ 152.9 (C-3′), 148.8 (C-7a), 146.2 (C-6), 142.1 (C-2′), 137.9 (C-4), 132.4 (C-3a), 126.0 (C-5′), 124.0 (C-6′), 122.2 (C-1′), 118.7(C-2), 116.0 (C-5), 112.9 (C-4′), 99.4 (C-3), 60.4 (C-11′), 55.8 (C-13′). APCI-HRMS *m/z*: calc. for $C_{15}H_{15}N_2O_2$ (MH^+), 255.1128, found 255.1129; Purity (HPLC): 100% (column: Venusil XBP C18(2) 4.6 mm ×150 mm; retention time: 5 min).

4-(4-Fluorophenyl)-1H-pyrrolo[2,3-b]pyridine ***(18e)***: compound was synthesised from 4-fluorophenylboronic acid and 4-chloro-7-azaindole in a yield of 34.10%, recrystallized from acetonitrile, pale yellow powder, mp 219.3–219.7 °C, Rf = 0.44 (2 petroleum ether: 1 ethyl acetate). ^{1}H NMR (DMSO-d_6, 600 MHz) δ 11.84 (1H, s, NH), 8.28 (1H, d, J = 4.9 Hz, H-6), 7.82 (2H, dd, J = 8.5, 5.6 Hz, H-2′, H-6′), 7.56 (1H, t, J = 3.0 Hz, H-2), 7.42–7.36 (2H, m, H-3′, H-5′), 7.18 (1H, d, J = 4.9 Hz, H-5), 6.60 (1H, d, J = 3.3 Hz, H-3). ^{13}C NMR (DMSO-d_6, 150 MHz) δ 162.7 (d, J = 245.5 Hz, C-4′), 149.6 (s, C-7a), 143.4 (s, C-6), 139.6 (s, C-5), 135.4 (d, J = 3.0 Hz, C-1′), 130.8 (d, J = 8.3 Hz, C-2′, C-6′), 127.2 (s, C-3a), 117.6 (s, C-2), 116.4 (d, J = 21.4 Hz, C-3′, C-5′), 114.7 (s, C-5), 99.3 (s, C-3). APCI-HRMS *m/z*: calc. for $C_{13}H_{10}FN_2$ (MH^+), 213.082253, found 213.0826; Purity (HPLC): 99% (column: Venusil XBP C18(2) 4.6 mm ×150 mm; retention time: 5 min).

4-(3,4-Difluorophenyl)-1H-pyrrolo[2,3-b]pyridine ***(18f)***: compound was synthesised from 3,4-difluorophenylboronic acid and 4-chloro-7-azaindole in a yield of 62.68%, recrystallized from acetonitrile, pale orange crystals, mp 172–174 °C, Rf = 0.20 (4 petroleum ether: 1 ethyl acetate). (DMSO-d_6, 600 MHz) δ 11.93 (1H, s, NH), 8.35 (1H, d, J = 4.8 Hz, H-6), 7.90–7.84 (1H, m, H-5′), 7.71–7.65 (2H, m, H-2′, H-4′), 7.64 (1H, t, J = 2.8 Hz, H-2), 7.26 (1H, d, J = 4.8 Hz, H-5), 6.68 (1H, m, H-3). ^{13}C NMR (DMSO-d_6, 150 MHz) δ 150.9 (dd, J = 33.0, 12.7 Hz, C-4′), 149.6 (s, C-7a), 149.3 (dd, J = 34.6, 12.5 Hz, C-3′), 143.4 (s, C-6), 138.4 (s, C-4), 136.5 (dd, J = 5.0, 4.3 Hz, C-1′), 127.6 (s, C-3a), 125.7 (dd, J = 6.5, 3.2 Hz, C-2′), 118.6 (d, J = 17.2 Hz, C-6′), 117.7 (d, J = 17.6 Hz, C-5′), 117.5 (s, C-2), 114.8 (s, C-5), 99.2 (s, C-3). APCI-HRMS *m/z*: calc. for $C_{13}H_9F_2N_2$ (MH^+), 231.0728, found 231.0736; Purity (HPLC): 98% (column: Venusil XBP C18(2) 4.6 mm ×150 mm; retention time: 4 min).

4-[4-(Trifluoromethyl)phenyl]-1H-pyrrolo[2,3-b]pyridine ***(18g)***: compound was synthesised from 4-trifluorophenyl boronic acid and 4-chloro-7-azaindole in a yield of 75.44%, recrystallized from acetonitrile, sand coloured crystals, mp 204–205 °C, Rf = 0.13 (4 petroleum ether: 1 ethyl acetate). ^{1}H NMR (DMSO-d_6, 600 MHz) δ 11.90 (1H, s, NH), 8.33 (1H, d, J = 4.8 Hz, H-6), 7.99 (2H, d, J = 7.9 Hz, H-3′, H-5′), 7.91 (2H, d, J = 7.9 Hz, H-2′, H-6′), 7.62–7.58 (1H, m, H-2), 7.26 (1H, d, J = 4.8 Hz, H-5), 6.65–6.62 (1H, m, H-3). ^{13}C NMR (DMSO-d_6, 150 MHz) δ 149.6 (s, C-7a), 143.5 (s, C-6), 143.0 (s, C-1′), 139.0 (s, C-4), 129.5 (s, C-3a), 129.1 (q, J = 31.7 Hz, C-4′), 127.7 (s, C-2′, C-6′), 126.3 (q, J = 3.6 Hz, C-3′, C-5′), 124.7 (d, J = 272.1 Hz, CF_3), 117.7 (s, C-2), 114.9 (s, C-5), 99.2 (s, C-3). APCI-HRMS *m/z*: calc. for $C_{14}H_{10}F_3N_2$ (MH^+), 263.0790, found 263.0798; Purity (HPLC): 99% (column: Venusil XBP C18 (2) 4.6 mm ×150 mm; retention time: 6 min).

4-(4-Chlorophenyl)-1H-pyrrolo[2,3-b]pyridine ***(18h)***: compound was synthesised from 4-chlorophenylboronic acid and 4-chloro-7-azaindole in a yield of 38.51%, recrystallized from acetonitrile, yellow powder, mp 222–223 °C, Rf = 0.24 (2 petroleum ether: 1 ethyl acetate). ^{1}H NMR (DMSO-d_6, 600 MHz) δ 11.81 (1H, s, NH), 8.29 (1H, d, J = 4.8 Hz, H-6), 7.79 (2H, d, J = 7.7 Hz, H-3′, H-5′), 7.60 (2H, d, J = 7.6 Hz, H-2′, H-6′), 7.57–7.55 (1H, m, H-2), 7.18 (1H, d, J = 4.8 Hz, H-2), 6.61–6.58 (1H, m, H-3). ^{13}C NMR (DMSO-d_6, 150 MHz) δ 149.6 (C-7a), 143.4 (C-6), 139.3 (C-1′), 137.7 (C-4), 133.6 (C-4′), 130.4 (C-3′, C-5′), 129.4 (C-2′, C-6′), 127.3 (C-3a), 117.5 (C-2), 114.6 (C-5), 99.3 (C-3). APCI-HRMS *m/z*: calc. for $C_{13}H_{10}ClN_2$ (MH^+), 229.0527, found 229.0537; Purity (HPLC): 83% (column: Venusil XBP C18(2) 4.6 mm ×150 mm; retention time: 6 min).

4-(Biphenyl-4-yl)-1H-pyrrolo[2,3-b]pyridine ***(18i)***: compound was synthesised from 4-biphenylboronic acid and 4-chloro-7-azaindole in a yield of 58.74%, recrystallized from acetonitrile, olive green powder, mp 266–267 °C, Rf = 0.43 (2 petroleum ether: 1 ethyl acetate). ^{1}H NMR (DMSO-d_6, 600 MHz) δ 11.81 (1H, s, NH), 8.30 (1H, d, J = 4.6 Hz, H-6), 7.88 (2H, d, J = 8.1 Hz, C-3′, C11′), 7.85 (2H, d, J = 7.6 Hz, C-2′, C12′), 7.76 (2H, d, J = 7.5 Hz, H-6′, H-10′), 7.56 (1H, d, J = 2.8 Hz, H-2), 7.51 (2H, t, J = 7.4 Hz, H-7′, H-9′), 7.41 (1H, t, J = 7.4 Hz, H-8′), 7.24 (1H, d, J = 4.6 Hz, H-5), 6.67 (1H, d, J = 2.2 Hz, H-3). ^{13}C NMR (DMSO-d_6, 150 MHz) δ 149.7 (C-7a), 143.4 (C-6), 140.5 (C-4′), 140.2 (C-5′), 140.0 (C-1′), 138.0 (C-4), 129.5 (C-7′, C-9′), 129.3 (C-3′, C-11′), 128.2 (C-3a), 127.7 (C2′, C12′), 127.3 (C8′), 127.2 (C-6′, C-10′), 117.7 (C-2), 114.6 (C-5), 99.5 (C-3). APCI-HRMS *m/z*: calc. for $C_{19}H_{15}N_2$ (MH^+),

271.1229, found 271.1224; Purity (HPLC): 89% (column: Venusil XBP C18(2) 4.6 mm × 150 mm; retention time: 5 min).

5-Phenyl-1H-pyrrolo[2,3-b]pyridine (***19a***): compound was synthesised from phenylboronic acid and 5-bromo-7-azaindole in a yield of 62.93%, recrystallized from ethanol, pale orange crystals, mp 160–162 °C, Rf = 0.57 (2 petroleum ether: 1 ethyl acetate). ^{1}H NMR (DMSO-d_6, 600 MHz) δ 11.71 (1H, s, NH), 8.52 (1H, d, J = 2.1 Hz, H-6), 8.21 (1H, d, J = 2.0 Hz, H-4), 7.71 (2H, d, J = 7.3 Hz, H-2′, H-6′), 7.53-7.51 (1H, m, H-2), 7.48 (2H, t, J = 7.6 Hz, H-3′, H-5′), 7.36 (1H, t, J = 7.3 Hz, H-4′), 6.52-6.50 (1H, m, H-3). ^{13}C NMR (DMSO-d_6, 150 MHz) δ 148.6 (C-7a), 142.0 (C-6), 139.6 (C-1′), 129.5 (C-5), 128.7 (C-3′, C-5′), 127.4 (C-4′), 127.4 (C-4), 127.3 (C-2′, C-6′), 126.6 (C-2), 120.2 (C-3a), 100.7 (C-3). APCI-HRMS *m/z*: calc. for $C_{13}H_{11}N_2$ (MH^+), 195.0916, found 195.0918; Purity (HPLC): 99% (column: Venusil XBP C18(2) 4.6 mm × 150 mm; retention time: 14 min).

5-(4-Methylphenyl)-1H-pyrrolo[2,3-b]pyridine (***19b***): compound was synthesised from *p*-tolylboronic acid and 5-bromo-7-azaindole in a yield of 59.94%, recrystallized from acetonitrile, brownish orange crystals, mp 182–184 °C, Rf = 0.71 (2 petroleum ether: 1 ethyl acetate). ^{1}H NMR (DMSO-d_6, 600 MHz) δ 11.71 (1H, s, NH), 8.49 (1H, d, J = 1.7 Hz, H-6), 8.16 (1H, d, J = 1.7 Hz, H-4), 7.59 (2H, d, J = 7.9 Hz, H-2′, H-6′), 7.51 (1H, t, J = 2.8 Hz, H-2), 7.28 (2H, d, J = 7.9 Hz, H-3′, H-5′), 6.52–6.47 (1H, m, H-3), 2.4 (3H, s, Me-4′). ^{13}C NMR (DMSO-d_6, 150 MHz) δ 148.4 (C-7a), 141.8 (C-6), 136.7 (C-4′), 136.5 (C-1′), 130.1 (C-5), 128.6 (C-3′, C-5′), 127.4 (C-4), 127.2 (C-2′, C-6′), 126.3 (C-2), 120.2 (C-3a), 100.6 (C-3), 21.1 (Me-4′). APCI-HRMS *m/z*: calc. for $C_{14}H_{13}N_2$ (MH^+), 209.1073, found 209.1071; Purity (HPLC): 87% (column: Venusil XBP C18(2) 4.6 mm × 150 mm; retention time: 11 min).

5-(3-Methoxyphenyl)-1H-pyrrolo[2,3-b]pyridine (***19c***): compound was synthesised from 3-methoxyphenylboronic acid and 5-bromo-7azaindole in a yield of 63.05%, recrystallized from acetonitrile, pale yellow crystals, mp 140–141 °C, Rf = 0.63 (2 petroleum ether: 1 ethyl acetate). ^{1}H NMR (DMSO-d_6, 600 MHz) δ 11.73 (1H, s, NH), 8.52 (1H, d, J = 2.1 Hz, H-6), 8.22 (1H, d, J = 2.1 Hz, H-4), 7.52 (1H, t, J = 2.9 Hz, H-2′), 7.39 (1H, td, J = 7.7, 08 Hz, H-5′), 7.28 (1H, dd, J = 5.8, 2.0 Hz, H-4′), 7.25–7.23 (1H, m, H-2), 6.93 (1H, dd, J = 8.2, 2.4 Hz, H-6′), 6.52 – 6.50 (1H, m, H-3), 3.8 (3H, s, Me-3′). ^{13}C NMR (DMSO-d_6, 150 MHz) δ 160.3 (C-3′), 148.6 (C-7a), 142.0 (C-6), 141.1 (C-1′), 130.5 (C-5), 128.5 (C-5′), 127.5 (C-6′), 126.7 (C-4), 120.1 (C-2), 119.7 (C-3a), 113.0 (C-4′), 112.7 (C-2′), 100.7 (C-3), 55.6 (Me-3′). APCI-HRMS *m/z*: calc. for $C_{14}H_{13}N_2O$ (MH^+), 225.1022, found 225.1030; Purity (HPLC): 69% (column: Venusil XBP C18(2) 4.6 mm × 150 mm; retention time: 8 min).

5-(4-Methoxyphenyl)-1H-pyrrolo[2,3-b]pyridine (***19d***): compound was synthesised from 4-methoxyphenylboronic acid and 5-bromo-7-azaindole in a yield of 82.70%, recrystallized from acetonitrile, mustard coloured crystals, mp 227–228 °C, Rf = 0.23 (2 petroleum ether: 1 ethyl acetate). ^{1}H NMR (DMSO-d_6, 600 MHz) δ 11.68 (1H, s, NH), 8.47 (1H, d, J = 1.9 Hz, H-6), 8.13 (1H, d, J = 1.8 Hz, H-4), 7.63 (2H, d, J = 8.1 Hz, H-3′, H-5′), 7.50 (1H, t, J = 3.1 Hz, H-2), 7.04 (2H, d, J = 8.1 Hz, H-2′, H-6′), 6.50–6.46 (1H, m, H-3), 3.80 (3H, s, Me-4′). ^{13}C NMR (DMSO-d_6, 150 MHz) δ 159.0 (C-4′), 148.2 (C-7a), 141.7 (C-6), 132.0 (C-1′), 128.4 (C-5), 127.7 (C-2′, C-6′), 127.3 (C-4), 126.0 (C-2), 120.2 (C-3a), 114.9 (C-3′, C-5′), 100.5 (C-3), 55.6 (MeO-4′). APCI-HRMS *m/z*: calc. for $C_{14}H_{13}N_2O$ (MH^+), 225.1022, found 225.1023; Purity (HPLC): 100% (column: Venusil XBP C18(2) 4.6 mm ×150 mm; retention time: 11 min).

5-(2,3-Dimethoxyphenyl)-1*H*-pyrrolo[2,3-*b*]pyridine (***19e***): compound was synthesised from 2,3-dimethoxyphenylboronic acid and 5-bromo-7-azaindole in a yield of 11.11%, recrystallized from acetonitrile, white crystals, mp 136–138 °C Rf = 0.36 (2 petroleum ether: 1 ethyl acetate). ^{1}H NMR ($CDCl_3$, 600 MHz) δ 10.19 (1H, s, NH), 8.54 (1H, d, J = 1.8 Hz, H-6), 8.15 (1H, d, J = 1.7 Hz, H-4), 7.39–7.37 (1H, m, H-2), 7.15 (1H, t, J = 7.9 Hz, H-5′), 7.02 (1H, dd, J = 7.7, 1.3 Hz, H-4′), 6.96 (1H, dd, J = 8.2, 1.2 Hz, H-6′), 6.56 (1H, dd, J = 3.3, 1.7 Hz, H-3), 3.94 (3H, s, Me-2′), 3.6 (3H, s, Me-3′). ^{13}C NMR ($CDCl_3$,151 MHz) δ 153.4 (C-3′), 148.0 (C-7a), 146.9 (C-6), 144.0 (C-2′), 134.2 (C-5), 129.7 (C-5′), 126.6 (C-6′), 125.4 (C-4), 124.4 (C-1′), 123.1 (C-2), 120.0 (C-3a), 111.7 (C-4′), 101.4 (C-3), 60.7 (MeO-2′), 56.1 (MeO-3′). APCI-HRMS m/z: calc. for $C_{15}H_{15}N_2O_2$ (MH^+), 255.1128, found 255.1130; Purity (HPLC): 99% (column: Venusil XBP C18(2) 4.6 mm × 150 mm; retention time: 6 min).

5-(3,4-Dimethoxyphenyl)-1H-pyrrolo[2,3-b]pyridine (***19f***): compound was synthesised from 3,4-dimethoxyphenylboronic acid and 5-bromo-7-azaindole in a yield of 46.25%, recrystallized from acetonitrile, yellow crystals, mp 210–211 °C, Rf = 0.18 (2 petroleum ether: 1 ethyl acetate). ^{1}H NMR (DMSO-d_6, 600 MHz) δ 11.68 (1H, s, NH), 8.51 (1H, d, J = 2.0 Hz, H-6), 8.18 (1H, d, J = 1.9 Hz, H-4), 7.50 (1H, t, J = 2.8 Hz, H-2), 7.27 (1H, d, J = 1.9 Hz, H-2′), 7.22 (1H, dd, J = 8.2, 2.0 Hz, H-5′), 7.05 (1H, d, J = 8.3 Hz, H-6′), 6.50–6.48(1H, m, H-3), 3.9 (3H, s, Me-3′), 3.8 (3H, s, Me-4′). ^{13}C NMR (DMSO-d_6, 150 MHz) δ 149.6 (C-7a), 148.5 (C-4′), 148.3 (C-3′), 141.9 (C-6), 132.4 (C-1′), 128.7 (C-5), 127.3 (C-6′), 126.2 (C-4), 120.1 (C-2), 119.3 (C-3a), 112.8 (C-5′), 111.2 (C-2′), 100.5 (C-3), 56.1 (MeO-3′), 56.0 (MeO-4′). APCI-HRMS *m/z*: calc. for $C_{15}H_{15}N_2O_2$ (MH^+), 255.1128, found 255.1124; Purity (HPLC): 100% (column: Venusil XBP C18(2) 4.6 mm ×150 mm; retention time: 11 min).

*5-(4-Fluorophenyl)-1H-pyrrolo[2,3-b]pyridine (**19g**)*: compound was synthesised from 4-fluorophenylboronic acid and 5-bromo-7-azaindole in a yield of 52.63%, recrystallized from acetonitrile, dark yellow crystals, mp 182–184 °C, Rf = 0.48 (2 petroleum ether: 1 ethyl acetate). ^{1}H NMR (DMSO-d_6, 600 MHz) δ 11.74 (1H, s, NH), 8.49 (1H, d, J = 2.2 Hz, H-6), 8.19 (1H, d, J = 2.1 Hz, H-4), 7.76–7.73 (2H, m, H-2′, H-6′), 7.53 (1H, t, J = 2.8 Hz, H-2), 7.32–7.29 (2H, m, H-3′, H-5′), 6.52–6.49 (1H, m, H-3). ^{13}C NMR (DMSO-d_6, 150 MHz) δ 162.1 (d, J = 243.6 Hz, C-4′), 148.5 (s, C-7a), 141.9 (s, C-6), 136.1 (d, J = 2.9 Hz, C-1′), 129.3 (d, J = 8.1 Hz, C-2′, C-6′), 127.7 (s, C-5), 127.5 (s, C-4), 126.6 (s, C-2), 120.1 (s, C-3a), 116.2 (d, J = 21.3 Hz, C-3′, C-5′), 100.6 (s, C-3). APCI-HRMS *m/z*: calc. for $C_{13}H_{10}FN_2$ (MH^+), 213.0822, found 213.0823; Purity (HPLC): 100% (column: Venusil XBP C18 (2) 4.6 mm × 150 mm; retention time: 8 min).

*5-(3,4-Difluorophenyl)-1H-pyrrolo[2,3-b]pyridine (**19h**)*: compound was synthesised from 3,4-difluorophenylboronic acid and 5-bromo-7-azaindole in a yield of 43.02%, recrystallized from acetonitrile, mustard coloured crystals, mp 194–196 °C, Rf = 0.47 (2 petroleum ether: 1 ethyl acetate). ^{1}H NMR (DMSO-d_6, 600 MHz) δ 11.79 (1H, s, NH), 8.53 (1H, d, J = 2.2 Hz, H-6), 8.24 (1H, d, J = 2.2 Hz, H-4), 7.83 (1H, ddd, J = 12.2, 7.8, 2.2 Hz, H-2′), 7.59–7.56 (1H, m, H-5′), 7.55–7.53 (1H, m, H-2), 7.53–7.49 (1H, m, H-6′), 6.52–6.50 (1H, m, H-3). ^{13}C NMR (DMSO-d_6, 150 MHz) δ 150.5 (dd, J = 157.2, 12.7 Hz, C-4′), 148.9 (dd, J = 157.2, 12.7 Hz, C-3′), 148.7 (s, C-7a), 141.9 (s, C-6), 137.3 (dd, J = 6.3, 3.6 Hz, C-1′), 127.7 (s, C-5), 126.8 (s, C-4), 126.5 (s, C-2), 123.9 (dd, J = 6.2, 3.1 Hz, C-6′), 120.1 (s, C-3a), 118.4 (d, J = 17.0 Hz, C-5′), 116.3 (d, J = 17.6 Hz, C-2′), 100.7 (s, C-3). APCI-HRMS *m/z*: calc. for $C_{13}H_9F_2N_2$ (MH^+), 231.0728, found 231.0724; Purity (HPLC): 100% (column: Venusil XBP C18(2) 4.6 mm × 150 mm; retention time: 9 min).

*5-[4-(Trifluoromethyl)phenyl]-1H-pyrrolo[2,3-b]pyridine (**19i**)*: compound was synthesised from 4-trifluorophenyl boronic acid and 5-bromo-7-azaindole in a yield of 52.88%, recrystallized from acetonitrile, pale yellow crystals, mp 236–237 °C, Rf = 0.50 (2 petroleum ether: 1 ethyl acetate). ^{1}H NMR (DMSO-d_6, 600 MHz) δ 11.84 (1H, s, NH), 8.59 (1H, d, J = 1.8 Hz, H-6), 8.31 (1H, d, J = 1.8 Hz, H-4), 7.96 (2H, d, J = 8.1Hz, H-3′, H-5′), 7.82 (2H, d, J = 8.1 Hz, H-2′, H-6′), 7.56 (1H, d, J = 3.2 Hz, H-2), 6.54 (1H, d, J = 3.3 Hz, H-3). ^{13}C NMR (DMSO-d_6, 150 MHz) δ 148.9 (s, C-7a), 143.7 (s, C-6), 142.1 (s, C-1′), 128.0 (s, C-5), 127.8 (s, C-4), 127.7 (d, J = 31.9 Hz, C-4′), 127.1 (d, J = 6.1 Hz, C-2′, C-6′), 126.3 (d, J = 6.1 Hz, C-3′, C-5′), 126.2 (s, C-2), 125.0 (d, J = 271.7 Hz, CF_3), 120.2 (s, C-3a), 100.9 (s, C-3). APCI-HRMS *m/z*: calc. for $C_{14}H_{10}F_3N_2$ (MH^+), 263.0790, found 263.0787; Purity (HPLC): 100% (column: Venusil XBP C18(2) 4.6 mm × 150 mm; retention time: 10 min).

*5-(4-Chlorophenyl)-1H-pyrrolo[2,3-b]pyridine (**19j**)*: compound was synthesised from 4-chlorophenylboronic acid and 5-bromo-7azaindole in a yield of 70.40%, recrystallized from acetonitrile, gold crystals, mp 195-197 °C, Rf = 0.41 (2 petroleum ether: 1 ethyl acetate). ^{1}H NMR (DMSO-d_6, 600 MHz) δ 11.77 (1H, s, NH), 8.52 (1H, d, J = 2.2 Hz, H-6), 8.22 (1H, d, J = 2.0 Hz, H-4), 7.76–7.73 (2H, m, H-2′, H-6′), 7.54–7.51 (3H, m, H-2, H-3′, H-5′), 6.52–6.50 (1H, m, H-3). ^{13}C NMR (DMSO-d_6, 150 MHz) δ 148.6 (C-7a), 141.9 (C-6), 138.5 (C-1′), 132.2 (C-4′), 129.4 (C-5), 129.1 (C-3′, C-5′), 127.6 (C-2′, C6′), 127.3 (C-4), 126.6 (C-2), 120.1 (C-3a), 100.7 (C-3). APCI-HRMS *m/z*: calc. for $C_{13}H_{10}ClN_2$ (MH^+), 229.0527, found 229.0536; Purity (HPLC): 100% (column: Venusil XBP C18(2) 4.6 mm × 150 mm; retention time: 8 min).

*4-(1H-Pyrrolo[2,3-b]pyridin-5-yl)benzonitrile (**19k**)*: compound was synthesised from 4-cyanoboronic acid and 5-bromo-7-azaindole in a yield of 33.53%, recrystallized from acetonitrile, pale yellow crystals, mp 287–293 °C, Rf = 0.38 (2 petroleum ether: 1 ethyl acetate). ^{1}H NMR (DMSO-d_6, 600 MHz) δ 11.85 (1H, s, NH), 8.61 (1H, d, J = 2.2 Hz, H-6), 8.33 (1H, d, J = 2.1 Hz, H-4), 7.95 (2H, d, J = 8.5 Hz, H-3′, H-5′), 7.93 (2H, d, J = 8.5 Hz, H-2′, H6′), 7.56 (1H, t, J = 3.3 Hz, H-2), 6.55–6.53 (1H, m, H-3). ^{13}C NMR (DMSO-d_6, 150 MHz) δ 149.0 (C-7a), 144.3 (C-6), 142.1 (C-1′), 133.3 (C-3′, C-5′), 128.0 (C-2′, C-6′), 127.9 (C-5), 127.2 (C-4), 126.7 (C-2), 120.2 (C-3a), 119.5 (CN), 109.8 (C-4′), 101.0 (C-3). APCI-HRMS *m/z*: calc. for $C_{14}H_{10}N_3$ (MH^+), 220.086924, found 220.0872; Purity (HPLC): 99% (column: Venusil XBP C18(2) 4.6 mm × 150 mm; retention time: 5 min).

*5-(Biphenyl-4-yl)-1H-pyrrolo[2,3-b]pyridine (**19l**)*: compound was synthesised from 4-biphenylboronic acid and 5-bromo-7-azaindole in a yield of 19.90%, recrystallized from acetonitrile, white powder, mp 264–265 °C, Rf = 0.36 (2 petroleum ether: 1 ethyl acetate). ^{1}H NMR (DMSO-d_6, 600 MHz) δ 11.76 (1H, s, NH), 8.59 (1H, d, J = 2.1 Hz, H-6), 8.27 (1H, d, J = 2.0 Hz, H-4), 7.82 (2H, d, J = 8.3 Hz, H-2, H-12′), 7.78 (2H, d, J = 8.4 Hz, H-3′, H-11′), 7.74 (2H, d, J = 7.3 Hz, H-6′, H-10′), 7.55–7.53 (1H, m, H-2), 7.50 (2H, t, J = 7.7 Hz, H-7′, H-9′), 7.39 (1H, t, J = 7.4 Hz, H-8′), 6.53 (1H, m, H-3). ^{13}C NMR (DMSO-d_6, 150 MHz) δ 148.6 (C-7a), 141.9 (C-6), 140.2 (C-4′), 139.0 (C-5′), 138.6 (C-1′), 129.5 (C-7′, C-9′), 128.1 (C-5), 127.9 (C-8′), 127.8 (C-3′, C-11′), 127.7 (C-2′, C-12′), 127.5 (C-4), 127.0 (C-6′, C10′), 126.5 (C-2), 120.2 (C-3a), 100.7 (C-3). APCI-HRMS *m/z*: calc. for $C_{19}H_{15}N_2$ (MH^+), 271.1229, found 271.1222; Purity (HPLC): 73% (column: Venusil XBP C18 (2) 4.6 mm × 150 mm; retention time: 7 min).

*5-(Pyridin-3-yl)-1H-pyrrolo[2,3-b]pyridine (**19m**)*: compound was synthesised from pyridin-3-ylboronic acid and 5-bromo-7-azaindole in a yield of 44.78%, recrystallized from acetonitrile and ethanol, yellow crystals, mp 176–177 °C, Rf = 0.07 (2 petroleum ether: 1 ethyl acetate).

^{1}H NMR (DMSO-d_6, 600 MHz) δ 11.81 (1H, s, NH), 8.95 (1H, d, $J = 1.9$ Hz, H-6), 8.58–8.55 (2H, m, C-2′, C-4′), 8.30 (1H, d, $J = 1.9$ Hz, H-4), 8.15–8.12 (1H, m, H-6′), 7.55 (1H, t, $J = 2.8$ Hz, H-2), 7.51–7.48 (1H, m, H-5′), 6.55–6.52 (1H, m, H-3). ^{13}C NMR (DMSO-d_6, 150 MHz) δ 100.8 (C-7a), 120.2 (C-2′), 124.4 (C-4′), 125.5 (C-6), 126.9 (C-6′), 127.7 (C-5), 134.7 (C-1′), 135.1 (C-4), 141.9 (C-2), 148.2 (C-5′), 148.4 (C-3a), 148.8 (C-3). APCI-HRMS *m/z*: calc. for $C_{12}H_{10}N_3$ (MH^+), 196.0869, found 196.0882; Purity (HPLC): 100% (column: Venusil XBP C18(2) 4.6 mm × 150 mm; retention time:7 min).

5-(Pyridin-4-yl)-1H-pyrrolo[2,3-b]pyridine (***19n***): compound was synthesised from pyridin-4-ylboronic acid and 5-bromo-7-azaindole in a yield of 45.12%, recrystallized from acetonitrile, yellow powder, mp 211.3–214.0 °C, Rf = 0.07 (2 petroleum ether: 1 ethyl acetate). ^{1}H NMR (DMSO-d_6, 600 MHz) δ 11.88 (1H, s, NH), 8.67 (1H, d, $J = 2.1$ Hz, H-6), 8.63 (2H, dd, J = 5.3, 1.3 Hz, H-3′, H-5′), 8.40 (1H, d, $J = 2.1$ Hz, H-4), 7.79 (2H, dd, $J = 5.6$, 1.5 Hz, H-2′, H-6′), 7.58–7.56 (1H, m, H-2), 6.57–6.54 (1H, m, H-3). ^{13}C NMR (DMSO-d_6, 150 MHz) δ 150.6 (C-7a), 149.3 (C-3′-C-5′), 146.6 (C-6), 141.9 (C-1′), 128.0 (C-5), 127.00 (C-4), 125.4 (C-2), 121.7 (C-2′, C-6′), 120.2 (C-3a), 101.0 (C-3). APCI-HRMS *m/z*: calc. for $C_{12}H_{10}N_3$ (MH^+), 196.0869, found 196.0886; Purity (HPLC): 99% (column: Venusil XBP C18 (2) 4.6 mm × 150 mm; retention time: 5 min).

5-(6-Fluoropyridin-3-yl)-1H-pyrrolo[2,3-b]pyridine (***19o***): compound was synthesised from 2-fluoropyridine-5-boronic acid and 5-bromo-7azaindole in a yield of 60.62%, recrystallized from acetonitrile, gold powder, mp 204–205 °C, Rf = 0.26 (2 petroleum ether: 1 ethyl acetate). ^{1}H NMR (DMSO-d_6, 600 MHz) δ 11.82 (1H, s, NH), 8.59 (1H, d, $J = 2.4$ Hz, H-6), 8.55 (1H, d, $J = 2.2$ Hz, H-4′), 8.36–8.32 (1H, m, H-5′), 8.28 (1H, t, $J = 2.3$ Hz, H-2), 7.56 (1H, s, H-2′), 7.30 (1H, dd, $J = 8.8$, 2.9 Hz, H-6′), 6.52 (1H, m, H-3). ^{13}C NMR (DMSO-d_6, 150 MHz) δ 162.8 (d, $J =$ 235.3 Hz, C-4′), 148.8 (s, C-7a), 145.8 (d, $J = 15.0$ Hz, C-2′), 141.9 (s, C-6), 140.9 (d, $J = 7.9$ Hz, C-1′), 133.7 (d, $J = 4.5$ Hz, C-6′), 127.8 (s, C-5), 126.9 (s, C-4), 124.4 (s, C-2), 120.1 (s, C-), 110.1 (d, $J = 37.7$ Hz, C-5′), 100.7 (s, C-3). APCI-HRMS *m/z*: calc. for $C_{12}H_9FN_3$ (MH^+), 214.077502, found 214.0791; Purity (HPLC): 99% (column: Venusil XBP C18(2) 4.6 mm × 150 mm; retention time: 4 min).

Protein kinase assays

Kinase activities were assayed in duplicate and described in Nguyen et al (Nguyen et al. 2019) except for the following enzymes: (i) *Lm*CK1 (from *Leishmania major*, recombinant, expressed in bacteria) was assayed in buffer A with 170 µM of the following CK1-specific peptide substrate: RRKHAAIGSpAYSITA ("Sp" stands for phosphorylated serine); (ii) *Ssc*CK1δ/ε (casein kinase 1δ/ε, porcine brain, native, affinity purified) was assayed in buffer A with 170 µM of the CK1-specific peptide substrate; (iii) *Ssc*GSK-3α/β (glycogen synthase kinase-3, porcine brain, native, affinity purified) isoforms were assayed in buffer A with 20 µM of GS-1 peptide, a GSK-3-selective substrate (YRRAAVPPSPSLSRHSSPHQSpEDEEE). Composition of buffer A: 10 mM $MgCl_2$, 1 mM EGTA, 1 mM DTT, 25 mM Tris-HCl pH 7.5, 50 µg/mL heparin. The peptides were obtained from Proteogenix (Oberhausbergen, France).

To measure the kinase activities, we used the ADP-Glo™ assay kit according to the recommendations of the manufacturer (Promega, Madison, WI). This assay is a luminescent ADP detection assay that provides an homogeneous and high-throughput screening method to measure kinase activity by quantifying the amount of ADP produced during a kinase reaction. Briefly, the reactions were carried out in 384-well plates in a final volume of 6 µl for 30 min at 30 °C in appropriate kinase buffer, with either protein or peptide as substrate in the presence of 10 µM ATP. After that, 6 µl of ADP-Glo™ Kinase Reagent was added to stop the kinase reaction. After an incubation time of 50 min at room temperature (RT), 12 µl of Kinase Detection Reagent was added for one hour at RT. The transmitted signal was measured using the Envision (PerkinElmer, Waltham, MA) microplate luminometer and expressed in Relative Light Unit (RLU). The compounds were first diluted at 10 mM in DMSO (stock solution) before to be analyzed as described hereafter. In this study, we used a two-step process to evaluate the effect of the 7-azaindole derivatives on kinase activity: (Step 1) As primary screening, the compounds were tested at 10 and 1 µM against a panel of eight disease-related kinases. Activities were expressed in % of maximal activity, i.e. measured with dimethyl sulfoxide (DMSO) diluted at 1% (v/v) concentration; (Step 2) The more active compounds (dubbed "hits") were next tested in duplicate over a wide range of concentrations (usually from 0.0003 to 10 µM) against the targets identified during "step 1", here Haspin and CDK9/CyclinT, and IC_{50} values were determined from the dose response curves using Prism-GraphPad (GraphPad Software, San Diego, CA, USA).

Cytotoxicity prediction

The cytotoxicity for the most promising compounds were predicted using CLC-Pred: in silico prediction of cytotoxicity for tumour and non-tumour cell-lines (Lagunin et al. 2018). CLC-Pred was developed by using the previously developed Prediction of Activity Spectra for Substances (PASS) algorithm to create and validate the classification structure-activity relationship (SAR) models for predicting

the cytotoxicity of structures against various types of human cell lines using ChEMBL experimental data. The experimental data from ChEMBL (IG_{50}, IC_{50} and % inhibition values) forms the basis for a training set of 59882 structures of compounds and the average accuracy of predicting area-under-the-curve (AUC) is given as 0.930 and 0.927 for 278 cancer cell-lines, when calculated by leave-one-out and 20-fold cross-validation procedure, respectively (Lagunin et al. 2018).

Results and discussion

7-Azaindole derivatives have been investigated against numerous PKs wherein they have exhibited good inhibition potentials (see Fig. 1). The inhibitory potential of this compound class against Haspin, a kinase with less similarity to those mentioned in Fig. 1, has not been investigated (Amoussou et al. 2018). Hence, in the current study a library of twenty-four 7-azaindole derivatives was synthesised and screened against Haspin. The compounds were also screened against a panel of other PKs. The screening panel consisted of kinases: ***Hs*CDK2/CyclinA**, ***Hs*CDK5/p25**, ***Hs*CDK9/CyclinT**, ***Hs*Haspin**, ***Hs*PIM1**, ***Ssc*CK1δ/ε**, ***Ssc*GSK3α/β** and ***Lm*CK1**. **Haspin** is of particular interest as a novel biological target with regards to these compounds.

Initially, the compounds were screened at concentrations of 10 and 1 μM (diluted in 1% DMSO v/v). Only the compounds exhibiting inhibition greater than 70% at 1 μM (as arbitrary threshold) underwent more thorough testing (at a wide range of concentrations, usually 0.0003 μM–10 μM) and IC_{50} values were determined by means of dose-response curves (Prism-GraphPad). The results of the in vitro kinase assays can be found in Table 3 and Table 4.

The 7-azaindole derivatives of this study proved to exhibit inhibitory activity against two of the eight PKs in the panel, namely, CDK9/Cyclin T and Haspin. Interestingly, the compounds that were deemed active (**18a**, **18b**, **18c**, **18e**, **18f**, **18h**, & **19n**) all belong to the 4-substituted 7-azaindole derivatives, with the exception of one 5-substituted 7-azaindole derivative, **19n**. Their 5-substituted 7-azaindole counterparts **19a**, **19b**, **19d**, **19g**, **19h** and **19j** lacked significant activity, thus, it can be postulated that substitution on the 4-position may greatly improve inhibition of CDK9/Cyclin T and Haspin. Moreover, active compounds seem to favour inhibition of CDK9/Cyclin T over Haspin with inhibition ranging from 0.063 μM (**18e**) ≤ IC_{50} ≤ 1.2 μM (**18h**) for CDK9/Cyclin T and 0.118 μM (**18c**) ≤ IC_{50} ≤ 1.016 μM (**18e**) for Haspin.

Considering solely the inhibitory activity for CDK9/CyclinT, the best results were achieved by substituting the 4-position of the 7-azaindole with a 4′-fluorophenyl substituent (**18e**), which exhibited inhibitory activity against CDK9/CyclinT of 0.063 μM, followed closely by substitution with an unsubstituted phenyl ring (**18a**), which also achieved sub-micromolar activity (0.081 μM). Comparison of the active 4-substituted 7-azaindoles with the 4-substituted compounds that did not exhibit significant activity, revealed that the molecular weight of the substituent (in addition to position of the substituent) may have an impact of inhibitory activity against CDK9/Cyclin T. The compounds deemed active all bear a substituent of low molecular weight (< 130 g/mol), where 130 g/mol per substituent is surpassed (**18d**, **18g**, **18i**), the compound has lower or insignificant inhibitory CDK9/Cyclin T activity in comparison to the active 4-substituted 7-azaindole derivatives. In conjunction with molecular weight, inhibitory activity for CDK9/Cyclin T may also be governed by the electronegativity of the substituent. Three compounds bearing comparable electronegative *para*-substituted phenyl rings were assessed, it was found that the more electronegative the atom (electronegativity: $\mathbf{F > OCH_3 > CH_3}$), the better the inhibitory activity of the compound (CDK9/CyclinT activity: **18e** > **18c** > **18b**) see Fig. 2. However, the impact exacted by molecular weight of substituents seems to outweigh the impact exacted by the electronegativity of substituents, as both **18g** and **18h** are highly electronegative, but exhibit only a poor activity and relatively low inhibitory activity (e.g. IC_{50} of 1.2 μM for 18 h). Haspin, like CDK9/Cyclin T, seems to favour the lower molecular weight 4-substituted 7-azaindole derivatives (**18b**, **18c**, **18e**, **18h**) with regards to inhibitory activity, with the exception of **18a** (substituted with an unsubstituted phenyl ring) which exhibits no significant inhibitory activity.

Regarding the cytotoxicity of the active compounds, the CLC-Pred prediction platform was used to predict the

Table 4 Kinase inhibitory activity of compounds selected after primary screening (compounds inhibiting >70% of the kinase activity at 1 μM). Activities were assessed in duplicate using 10 μM ATP

Cpd	*Hs*CDK9/CyclinT	*Hs*Haspin
18a	**0.081**	NP
18b	**0.481**	**0.221**
18c	**0.206**	**0.118**
18e	**0.063**	**1.016**
18f	**0.137**	NP
18h	**1.200**	**0.284**
19n	NP	**0.664**
Flavopiridol	**0.015**	**NP**
CHR-6494	**NP**	**0.055**

Values represent IC_{50} reported in μM. Kinase activities were assessed in duplicate

NP Not performed

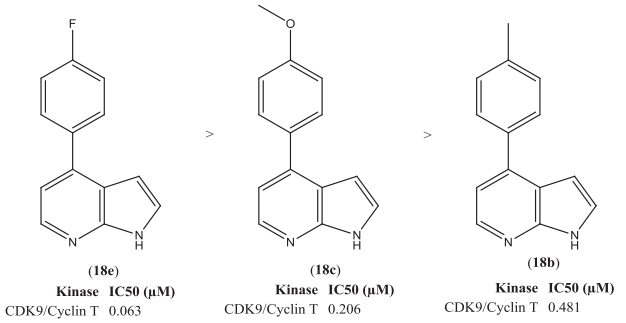

Fig. 2 Examples of 7-azaindole derivatives showing the significance of substitution with a more electronegative substituent in the para-position of the phenyl ring

cytotoxicity of these compounds (Lagunin et al. 2018). All of the active compounds (**18a**, **18b**, **18c**, **18e**, **18f**, **18h**, & **19n)** were predicted to have a cytotoxicity score higher than at least 60% of the compounds in the training set for oligodendrogliomas (Hs 683). Compound **18h**, exhibited the highest predicted cytotoxicity score (0.787), meaning that **18h** can be expected to be more cytotoxic against oligodendrogliomas than 78.7% of the compounds in the training set. Remarkably, the only active compound from the second series **19n**, is also the only active compound that is predicted to have cytotoxic activity against more than one cell-line, oligodendroglioma and malignant melanoma (Hs 683: 0.683 and A-375: 0.545) (see Table 5).

Overall, 7 active inhibitors of CDK9/Cyclin T and/or Haspin have been identified (**18a**, **18b**, **18c**, **18e**, **18f**, **18h**, & **19n**) with a high likelihood of being active against oligodendrogliomas. Thus, these compounds may have value as potential antimitotic agents in cancer therapy.

Conclusions

This article describes the synthesis of selected 4-, and 5-substituted azaindole derivatives, formed by the combination of the 7-azaindole scaffold and appropriate boronic acids. Protein kinase assays unveiled seven promising compounds; two compounds exhibited selective activity against CDK9/Cyclin T and one compound selectively against Haspin, while four compounds were identified as dual-target inhibitors of both CDK9/Cyclin T and Haspin, all with IC_{50} values in a nanomolar to low micromolar range. Furthermore, compound **18c** not only proved to be the most potent of the target inhibitors, but also, when considered separately, was identified as the compound with the best Haspin inhibitory activity (IC_{50} value of 0.118 μM against Haspin and 0.206 μM against CDK9/Cyclin T). Regarding CDK9/Cyclin T, compound **18e** reigned supreme with an IC_{50} value of 0.063 μM. Both Haspin and CDK9/Cyclin T, have been connected to normal cell proliferation and have been identified as targets in cancer therapy, thus compounds **18a**, **18b**, **18c**, **18e**, **18f**, **18h** and **19n** may potentially be of value as novel anti-proliferative agents (Huertas et al. 2012; Walsby et al. 2014). Furthermore, it is postulated that compound **18c** will make an excellent lead compound for further exploration of 7-azaindole derivatives as Haspin inhibitors.

Table 5 Predicted cytotoxicity most promising compounds (compounds inhibiting >70% of the kinase activity at 1 μM)

Cpd	Probability to be active (Pa)	Cell-line	Cell-line full name
18a	**0.721**	Hs 683	Oligodendroglioma
18b	**0.636**	Hs 683	Oligodendroglioma
18c	**0.652**	Hs 683	Oligodendroglioma
18e	**0.759**	Hs 683	Oligodendroglioma
18f	**0.734**	Hs 683	Oligodendroglioma
18h	**0.787**	Hs 683	Oligodendroglioma
19n	**0.638**	Hs 683	Oligodendroglioma
	0.545	A-375	Malignant melanoma
Flavopiridol	**0.509**	MRC5	Embryonic lung fibroblast (non-tumour cell-line)
CHR-6494	**0.385**	A-375	Malignant melanoma
	0.328	PA-1	Ovarian carcinoma
	0.319	SJSA-1	Osteosarcoma
	0.317	RKO	Colon carcinoma
	0.338	Kasumi 1	Childhood acute
	0.368	DMS-114	myeloid leukaemia with
	0.357	NCI-H838	maturation
	0.303	SK-MEL-1	Lung carcinoma
	0.307	MDA-MB-453	Non-small cell lung cancer Metastatic melanoma Breast carcinoma

Pa values represent the percentage of active compounds (from the training set) that is predicted to have a lower cytotoxicity for a specific cell-line than the investigated compound (Lagunin et al. 2018)

Acknowledgements The authors are grateful to Dr. D.Otto and Dr. J. Jordaan of the SASOL Centre for Chemistry, North-West University, for recording the MS and NMR spectra, respectively. The authors thank the "Ligue contre le Cancer du Grand-Ouest" comity, (districts: 29, 22, 56, 35, 45, and 79), Cancéropôle Grand Ouest (axis: natural sea products in cancer treatment network), IBiSA (French Infrastructures en sciences du vivant: biologie, santé et agronomie) and Biogenouest (Western France life science and environment core facility network) for supporting the KISSf screening facility (FR2424, CNRS and Sorbonne Université), Roscoff, France.

Compliance with ethical standards

Conflict of interest Stéphane Bach is a founder and member of the SAB of SeaBeLife Biotech (Roscoff, France). This company is developing novel therapies for treating liver and kidney acute disorders. This work was conducted in the absence of any commercial or

financial relationships that could be construed as a potential conflict of interest. The authors declare that they have no conflict of interest

Publisher's note Springer Nature remains neutral with regard to jurisdictional claims in published maps and institutional affiliations.

References

Allegretti M, Arcadi A, Marinelli F, Nicolini L (2001) Palladium-catalysed functionalisation at 4-and 6-position of the 7-azaindole system. Synlett 5:0609–0612

Amoussou NG, Bigot A, Roussakis C, Robert J-MH (2018) Haspin: a promising target for the design of inhibitors as potent anticancer drugs. Drug Discov Today 23:409–415

Arnold LD, Chen X, Dong H, Garton A., Mulvihill MJ, Smith CPS, Thomas GH, Krulle TM, Wang J. (2007) Fused heterobicyclic kinase inhibitors. US20070208053A1. Accessed from https://patents.google.com/patent/US20070208053A1/en on 06/05/2020

Bavetsias V, Faisal A, Crumpler S, Brown N, Kosmopoulou M, Joshi A, Atrash B, Pérez-Fuertes Y, Schmitt JA, Boxall KJ (2013) Aurora isoform selectivity: design and synthesis of imidazo [4, 5-b] pyridine derivatives as highly selective inhibitors of Aurora-A kinase in cells. J Med Chem 56:9122–9135

Cohen P (2002) Protein kinases—the major drug targets of the twenty-first century? Nat Rev Drug Discov 1:309–315

Dai J, Sultan S, Taylor SS, Higgins JM (2005) The kinase haspin is required for mitotic histone H3 Thr 3 phosphorylation and normal metaphase chromosome alignment. Genes Dev 19:472–488

Dai J, Sullivan BA, Higgins JM (2006) Regulation of mitotic chromosome cohesion by Haspin and Aurora B. Dev Cell 11:741–750

de Cárcer G, Perez de Castro I, Malumbres M (2007) Targeting cell cycle kinases for cancer therapy. Curr Med Chem 14:969–985

Duong-Ly KC, Peterson JR (2013) The human kinome and kinase inhibition. Curr Protoc Pharmacol 60:2.9. 1–2.9. 14

Fedorov O, Müller S, Knapp S (2010) The (un) targeted cancer kinome. Nat Chem Biol 6:166–169

Flight MH (2013) Neurodegenerative diseases: new kinase targets for Alzheimer's disease. Nat Rev Drug Discov 12:739

Gourdain SP, Dairou J, Denhez Cm, Bui LC, Rodrigues-Lima F, Janel N, Delabar JM, Cariou K, Dodd RH (2013) Development of DANDYs, new 3, 5-diaryl-7-azaindoles demonstrating potent DYRK1A kinase inhibitory activity. J Med Chem 56:9569–9585

Gummadi VR, Rajagopalan S, Looi C-Y, Paydar M, Renukappa GA, Ainan BR, Krishnamurthy NR, Panigrahi SK, Mahasweta K, Raghuramachandran S (2013) Discovery of 7-azaindole based anaplastic lymphoma kinase (ALK) inhibitors: wild type and mutant (L1196M) active compounds with unique binding mode. Bioorg Med Chem Lett 23:4911–4918

Hanks SK, Hunter T (1995) Protein kinases 6. The eukaryotic protein kinase superfamily: kinase (catalytic) domain structure and classification. The FASEB J 9:576–596

Harrington PE, Bourbeau MP, Fotsch C, Frohn M, Pickrell AJ, Reichelt A, Sham K, Siegmund AC, Bailis JM, Bush T (2013) The optimization of aminooxadiazoles as orally active inhibitors of Cdc7. Bioorg Med Chem Lett 23:6396–6400

Heinrich T, Seenisamy J, Emmanuvel L, Kulkarni SS, Bomke Jr, Rohdich F, Greiner H, Esdar C, Krier M, Grädler U (2013) Fragment-based discovery of new highly substituted 1 H-pyrrolo [2, 3-b]-and 3 H-imidazolo [4, 5-b]-pyridines as focal adhesion kinase inhibitors. J Med Chem 56:1160–1170

Higgins J (2003) Structure, function and evolution of haspin and haspinrelated proteins, a distinctive group of eukaryotic protein kinases. CMLS 60:446–462

Higgins JM (2001a) The Haspin gene: location in an intron of the Integrin αE gene, associated transcription of an Integrin αE-derived RNA and expression in diploid as well as haploid cells. Gene 267:55–69

Higgins JM (2001b) Haspin-like proteins: a new family of evolutionarily conserved putative eukaryotic protein kinases. Protein Sci 10:1677–1684

Higgins JM (2010) Haspin: a newly discovered regulator of mitotic chromosome behavior. Chromosoma 119:137–147

Hong S, Kim J, Seo JH, Jung KH, Hong S-S, Hong S (2012) Design, synthesis, and evaluation of 3, 5-disubstituted 7-azaindoles as Trk inhibitors with anticancer and antiangiogenic activities. J Med Chem 55:5337–5349

Huang Z, Tremblay MS, Wu TY-H, Ding Q, Hao X, Baaten J, Hill R, Liu B, Meeusen S, Zou Y (2019) Discovery of 5-(3, 4-Difluorophenyl)-3-(pyrazol-4-yl)-7-azaindole (GNF3809) for β-Cell Survival in Type 1 Diabetes. ACS Omega 4:3571–3581

Huertas D, Soler M, Moreto J, Villanueva A, Martinez A, Vidal A, Charlton M, Moffat D, Patel S, McDermott J (2012) Antitumor activity of a small-molecule inhibitor of the histone kinase Haspin. Oncogene 31:1408–1418

Hunter T (1995) Protein kinases and phosphatases: the yin and yang of protein phosphorylation and signaling. Cell 80:225–236

Huse M, Kuriyan J (2002) The conformational plasticity of protein kinases. Cell 109:275–282

Ibrahim PN, Artis DR, Bremer R, Habets G, Mamo S, Nespi M, Zhang C, Zhang J, Zhu Y, Zuckerman R (2007) Pyrrolo [2, 3-b] pyridine derivatives as protein kinase inhibitors. Int. Pat. Appl. Accessed from https://patents.google.com/patent/EP2395004A2/ko on 06/05/2020

Irie T, Sawa M (2018) 7-Azaindole: a versatile scaffold for developing kinase inhibitors. Chem Pharm Bull 66:29–36

Kannan N, Taylor SS, Zhai Y, Venter JC, Manning G (2007) Oceanic metagenomics: structural and functional diversity of the microbial kinome. PLoS Biol 5:e17

Kim KS, Zhang L, Schmidt R, Cai Z-W, Wei D, Williams DK, Lombardo LJ, Trainor GL, Xie D, Zhang Y (2008) Discovery of pyrrolopyridine—pyridone based inhibitors of Met kinase: Synthesis, X-ray crystallographic analysis, and biological activities. J Med Chem 51:5330–5341

Kim S-W, Kim M, Lee WY, Hyeon T (2002) Fabrication of hollow palladium spheres and their successful application to the recyclable heterogeneous catalyst for Suzuki coupling reactions. J Am Chem Soc 124:7642–7643

Lagunin AA, Dubovskaja VI, Rudik AV, Pogodin PV, Druzhilovskiy DS, Gloriozova TA, Filimonov DA, Sastry NG, Poroikov VV (2018) CLC-Pred: a freely available web-service for in silico prediction of human cell line cytotoxicity for drug-like compounds. PLoS One 13:e019183

Lawson M, Rodrigo J, Baratte B, Robert T, Delehouzé C, Lozach O, Ruchaud S, Bach S, Brion J-D, Alami M (2016) Synthesis, biological evaluation and molecular modeling studies of imidazo [1, 2-a] pyridines derivatives as protein kinase inhibitors. Eur J Med Chem 123:105–114

Ledeboer MW, Wannamaker M, Farmer L (2006). Pyrrolopyridines useful as inhibitors of protein kinase and their preparation, pharmaceutical compositions. and use in the treatment of various diseases, WO2006127587A1

Liao JJ-L (2007) Molecular recognition of protein kinase binding pockets for design of potent and selective kinase inhibitors. J Med Chem 50:409–424

Liddle J, Bamborough P, Barker MD, Campos S, Cousins RP, Cutler GJ, Hobbs H, Holmes DS, Ioannou C, Mellor GW (2009) 4-Phenyl-7-azaindoles as potent and selective IKK2 inhibitors. Bioorg Med Chem Lett 19:2504–2508

Littke AF, Fu GC (2002) Palladium-catalyzed coupling reactions of aryl chlorides. Angew Chem Int Ed 41:4176–4211

Liu B, Yuan X, Xu B, Zhang H, Li R, Wang X, Ge Z, Li R (2019) Synthesis of novel 7-azaindole derivatives containing pyridin-3-ylmethyl dithiocarbamate moiety as potent PKM2 activators and PKM2 nucleus translocation inhibitors. Eur J Med Chem 170:1–15

Manning G, Whyte DB, Martinez R, Hunter T, Sudarsanam S (2002) The protein kinase complement of the human genome. Science 298:1912–1934

Mavunkel BJ, Perumattam JJ, Tan X, Luedtke GR, Lu Q, Lim D, Kizer D, Dugar S, Chakravarty S, Xu Y-j (2010) Piperidine-based heterocyclic oxalyl amides as potent p38α MAP kinase inhibitors. Bioorg Med Chem Lett 20:1059–1062

Mérour J-Y, Buron F, Plé K, Bonnet P, Routier S (2014) The azaindole framework in the design of kinase inhibitors. Molecules 19:19935–19979

Metz JT, Johnson EF, Soni NB, Merta PJ, Kifle L, Hajduk PJ (2011) Navigating the kinome. Nat Chem Biol 7:200–202

Nakano H, Saito N, Parker L, Tada Y, Abe M, Tsuganezawa K, Yokoyama S, Tanaka A, Kojima H, Okabe T (2012) Rational evolution of a novel type of potent and selective proviral integration site in Moloney murine leukemia virus kinase 1 (PIM1) inhibitor from a screening-hit compound. J Med Chem 55:5151–5164

Nguyen T-N-D, Feizbakhsh O, Sfecci E, Baratte B, Delehouzé C, Garcia A, Moulin C, Colas P, Ruchaud S, Mehiri M (2019) Kinase-based screening of marine natural extracts leads to the identification of a cytotoxic high molecular weight metabolite from the mediterranean sponge crambe tailliezi. Mar Drugs 17: e569

Noh H, King G (2007) The role of protein kinase C activation in diabetic nephropathy. Kidney Int Suppl 72:S49–S53

Schmidt M, Bastians H (2007) Mitotic drug targets and the development of novel anti-mitotic anticancer drugs. Drug Resist Updat 10:162–181

Tsou H-R, MacEwan G, Birnberg G, Grosu G, Bursavich MG, Bard J, Brooijmans N, Toral-Barza L, Hollander I, Mansour TS (2010) Discovery and optimization of 2-(4-substituted-pyrrolo [2, 3-b] pyridin-3-yl) methylene-4-hydroxybenzofuran-3 (2H)-ones as potent and selective ATP-competitive inhibitors of the mammalian target of rapamycin (mTOR). Bioorg Med Chem Lett 20:2321–2325

Walsby E, Pratt G, Shao H, Abbas AY, Fischer PM, Bradshaw TD, Brennan P, Fegan C, Wang S, Pepper C (2014) A novel Cdk9 inhibitor preferentially targets tumor cells and synergizes with fludarabine. Oncotarget 5:375–385

Wolfe JP, Buchwald SL (1999) A highly active catalyst for the room-temperature amination and Suzuki coupling of aryl chlorides. Angew Chem Int Ed 38:2413–2416

Zhang C, Ibrahim PN, Zhang J, Burton EA, Habets G, Zhang Y, Powell B, West BL, Matusow B, Tsang G (2013) Design and pharmacology of a highly specific dual FMS and KIT kinase inhibitor. PNAS 110:5689–5694

Zuccotto F, Ardini E, Casale E, Angiolini M (2009) Through the "gatekeeper door": exploiting the active kinase conformation. J Med Chem 53:2681–2694